Bull. astr. Soc. India (1981) 9, 170–180

NOTES FOR THE OBSERVER

by T. P. Prabhu

1. Lunar occultations

Lunar occultations of bright stars predicted for Kavalur for the period between 1981 July–September are listed in Table 1. This list is more extensive than the list in the previous issue, since all stars to a limiting magnitude of 7.5 have been included. Some of these may be difficult targets particularly when the moon is very bright. Several naked eye stars being occulted in August–September are also close to the full moon. The occultation of χ^1 Orionis on September 20 is at the bright limb as one would note from the decreasing percentage illumination (negative sign in the last column of Table 1). Some occultations are rather early in the evening or early in the morning and may be troubled by twilight, while some others occur when the moon is too low. The easiest occultation of the quarter is that of γ Librae on August 8.

The predicted times listed in Table 1 have been computed for Kavalur. The times would be different for observers at other geographical locations. As in a total solar eclipse the shadow of the moon due to the star being occulted crosses the earth from west to east. The occultation is visible only in this path of the shadow. The actual times of appearance and disappearance are the same as the times when the shadow reaches an observer and leaves him. In the following is described a graphical method which can be used by any observer to ascertain whether a particular occultation would take place in his geographical location and to predict the accurate times of appearance and disappearance in the case the event takes place. Those who have access to an almanac and a star catalogue can utilize this method to predict new occultations for their geographical locations.

Since the moon is a close neighbour of the earth, its parallax is quite large. The maximum horizontal parallax of the moon is little over a degree. Therefore the position of the moon with respcct to the stars as seen by an observer may differ from the position as seen from the centre of the earth by a quantity which is little over one degree at its largest. Thus a coincidence between the geocentric position of the moon and that of a star does not ensure that an occultation is observable by every observer. Figure 1 illustrates this fact. Assume that δ_1 is the (geocentric) declination of the moon tabulated in the almanac and that star 1 has also the same declination. The shadow of the moon due to this star is centred at O_2 whose latitude is equal to the declination δ_1. The observer at O_1 (latitude ϕ) is outside this shadow and therefore does not see the occultation of star 1. On the other hand, he is at the centre of the shadow due to star 2 at δ_3 and witnesses the occultation of this star. There is a region of overlap of the two shadows where both the occultations would be visible.

The normal practice in the prediction of lunar occultations is to pick the candidate stars from a search range of $1\frac{1}{3}$ degree width in declination (see *Spherical Astronomy* by W. M. Smart). The generalization of the geometry of Figure 1 to

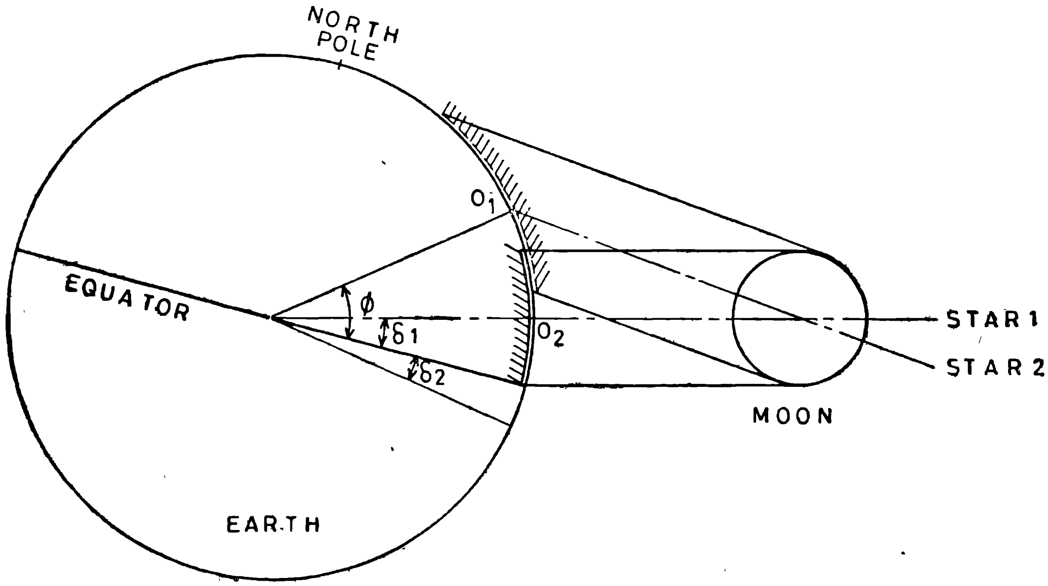

Figure 1. The shadow of the moon due to two stars : (a) Star 1 at the same declination as the moon ($\delta_1 = \phi_1$, solid line) and (b) Star 2 which is at a different declination (δ_2, broken line).

three dimensions helps us restrict the search range to just one lunar diameter ($\sim$ 32 arcmin) centred at the declination

$$\delta_2 = \delta_1 - p_1(\cos \delta_1 \sin \phi - \sin \delta_1 \cos \phi \cos h) \qquad ...(1)$$

where δ_1 is the tabulated lunar declination, p_1 is the maximum horizontal parallax and h is the hour angle of the moon. Note that the value of p_1 should be in the same units as that of δ and a value of 1° is sufficiently accurate for the purpose of defining the search range. Figure 1 corresponds to the moon on the meridian ($h = 0$) and consequently we have

$$\delta_2 = \delta_1 - p_1 \sin (\phi - \delta_1)$$

while for the rising and the setting moon ($h = 90°$) we have

$$\delta_2 = \delta_1 - p_1 \cos \delta_1 \sin \phi.$$

The value of δ_2 will be intermediate for intermediate value of h.

The procedure that we follow in the computation of the accurate times of immersion (or disappearance) and emersion (or reappearance) is described by Smart in his book mentioned above. The method consists of computing the position of the observer with respect to the shadow of the moon as seen projected on a plane perpendicular to the line joining the moon and the star at a given instant, and passing through the centre of the earth. This plane is called the *fundamental plane*. The zero point in time is generally taken to be the closest hour to the time when the right ascensions of the star and that of the moon coincide. One can easily obtain this hour by scanning through the hourly position of the moon in the *Indian Ephemeris* and comparing it with the position of the candidate star. Table 2 lists the quantities needed in such computations at a few specific instants of time. The times are so chosen as to be useful for an improvement of Table 1 for a location different from Kavalur. Note that the time in column 2 is referred to the Universal Time (UT) which is 5½ hours slower than the Indian Standard Time (IST).

Table 1. Lunar Occultations from 1981 July to October

Date		Time (UT) h	m	s	Type	Star	Mag.	SpT	α (1981) h	m	s	δ °	′	″	Altitude	Percentage illumination
July	4	13	20	26	D	HR 3736	6.3	K0	9	24	29	+16	40	04	32	10+
		14	10	45	R										20	
	7	17	39	32	D	BD + 4°2569	7.2	K0	12	03	45	+ 3	40	43	3	36+
	11	16	58	03	D	BD − 12°4198	7.3	A0	15	05	33	− 12	50	04	46	74+
		19	52	07	D	BD − 12°4214	7.5	K0	15	10	12	− 12	59	00	8	75+
	12	19	00	27	D	BD − 15°4221	6.8	M0	15	56	02	− 15	58	47	28	82+
	13	17	12	35	D	BD − 18°4315	7.2	K0	16	42	12	− 18	30	21	54	89+
	15	23	20	26	D	HR 6988	5.8	A5	18	36	49	− 21	24	45	2	98+
	16	20	02	52	D	BD − 21°5388	7.5	K2	19	25	22	− 21	16	55	49	100+
August	8	15	13	47	D	γ Librae	4.0	K0	15	34	29	−14	43	37	49	58+
		16	45	12	R										30	
	9	17	36	38	D	BD − 17°4572	7.2	F8	16	25	57	− 17	43	34	28	68+
	11	15	58	45	D	HR 6762	6.2	B1	18	06	05	− 21	26	44	55	84+
		17	08	03	D	BD − 21°4866	6.6	A2p	18	07	32	− 21	27	07	49	84+
		20	24	03	D	μ Sagittarii	4.0	B8p	18	12	40	− 21	03	48	12	85+
	12	18	21	10	D	BD − 21°5233	6.9	G0	19	03	15	− 21	33	30	45	91+
		21	54	17	D	π Sagittarii	3.0	F2	19	08	41	− 21	03	09	3	91+
	14	14	07	55	D	BD − 19°59	6.8	F5	20	47	11	− 19	19	39	25	99+
		18	14	47	D	BD −19°5954	7.5	G0	20	53	03	− 19	03	54	28	99+
		18	33	58	D	BD −19°5960	6.7	F0	20	53	45	− 18	51	44	58	99+
August	15	16	30	43	D	δ Capricorni	3.0	A5	21	46	02	− 16	12	36	44	100−
		17	47	42	R										57	
	18	20	20	06	D	BD − 2°0069	6.8	A0	00	30	44	− 1	53	41	68	88−
		20	35	07	R										71	

September	2	14	45	04	D	BD − 5°3758	7.5	K0	13	43	58	− 5	54	25	13	16+
	3	13	24	44	D	BD − 9°3945	6.7	K0	14	27	31	− 9	55	10	39	23+
		14	12	28	R										28	
	6	16	40	12	D	BD − 19°4471	6.1	B8	16	55	58	− 19	30	36	22	51+
	7	16	15	15	D	BD − 20°4874	7.1	A3	17	48	21	− 20	49	29	36	60+
	9	13	38	38	D	HR 7410	6.0	A2	19	29	49	− 21	21	01	51	78+
		14	41	55	D	BD − 21°5425	7.1	F5	19	31	10	− 21	33	21	56	78+
	11	22	26	45	D	BD − 16°5885	7.1	F5	21	32	40	− 16	16	53	3	94+
	13	15	42	19	D	BD − 10°6082	7.0	K0	23	12	02	− 9	40	10	44	100+
		17	56	26	D	ψ^1 Aquarii	4.5	K0	23	14	56	− 8	08	47	67	100+
		19	24	33	R										44	
	20	19	02	52	D	χ^1 Orionis	4.6	F8	5	53	17	+ 20	16	23	10	50 −
		19	24	08	R										15	
	23	22	45	08	D	BD + 18°2090	6.6	A0	8	57	14	+18	22	51	21	18 −
		23	57	03	R										38	
		23	23	00	D	HR 3577	6.6	M3	8	58	07	+18	12	29	30	17 −
	24	00	22	02	R										44	
	30	13	18	42	D	BD − 7°3794	7.1	K0	14	12	18	− 8	21	18	13	5+
		14	08	47	R										1	
October	3	15	24	56	D	BD − 18°4302	7.2	K0	16	37	29	− 18	47	15	12	25+
	6	15	34	46	D	HR 7276	6.4	K0	19	11	22	− 21	41	21	38	53+
	7	17	56	32	D	BD − 21°5629	7.3	F2	20	08	29	− 20	38	50	21	63+
		18	50	28	D	BD − 20°5836	7.3	K0	20	10	07	− 20	19	12	9	64+
	9	16	44	01	D	BD − 15°6092	7.0	K0	21	54	01	− 15	20	41	56	82+
		18	20	43	D	BD − 15°6103	7.2	A2	21	56	48	− 15	12	38	39	82+
	21	21	09	16	D	8 Leonis	5.9	K0	9	36	01	+16	31	17	15	31−
		22	18	14	R										32	

Table 2. Lunar ephemeris and the sidereal time

Date		UT	p_1	$\Delta p_1/\Delta t$	α_1			$\Delta\alpha_1/\Delta t$	δ_1			$\Delta\delta_1/\Delta t$	GST		
		h	arcsec	arcsec h^{-1}	h	m	s	sh^{-1}	°	′	″	arcsec h^{-1}	h	m	s
July	4	13	3482	−2.2	9	26	02	138	+16	42	36	−464	7	49	49
	7	18	3332	−1.6	12	07	41	116	+ 4	03	23	−658	13	02	28
	11	17	3250	0.0	15	07	12	116	−12	16	44	−528	12	18	04
		20	3250	0.0	15	13	00	116	−12	42	55	−519	15	18	34
	12	19	3255	+0.4	15	58	09	120	−15	47	00	−438	14	22	20
	13	17	3267	+0.7	16	42	50	124	−18	10	34	−342	12	25	57
	15	23	3315	+1.2	18	38	50	133	−21	06	08	− 33	18	34	49
	16	20	3341	+1.3	19	25	44	135	−20	53	37	+105	15	38	17
August	8	15	3255	+0.1	15	34	51	118	−14	16	47	−482	12	08	08
	9	18	3263	+0.5	16	28	46	122	−17	30	02	−373	15	12	34
	11	16	3304	+1.2	18	05	46	131	−20	46	15	−127	13	20	07
		20	3309	+1.2	18	14	30	131	−20	53	54	−103	17	20	47
	12	18	3337	+1.4	19	03	15	134	−21	05	51	+ 39	15	24	24
		22	3343	+1.4	19	12	13	135	−21	02	21	+ 66	19	25	03
	14	14	3405	+1.6	20	42	45	136	−18	48	30	+334	11	31	37
	14	18	3411	+1.6	20	51	49	136	−18	25	20	+360	15	32	17
	15	17	3446	+1.5	21	43	46	135	−15	40	04	+499	14	35	54
	18	20	3533	+0.6	0	29	19	131	− 1	58	07	+757	17	48	23
September	2	15	3292	+0.9	13	47	11	114	− 5	33	01	−637	13	46	42
	3	14	3267	−0.6	14	30	58	115	− 9	28	16	−587	12	50	29
	6	17	3264	+0.6	16	59	13	124	−19	00	59	−299	16	02	48
	7	16	3283	+1.1	17	47	32	128	−20	32	12	−174	15	06	35
	9	14	3345	+1.7	19	28	15	134	−20	57	27	+116	13	14	08
	11	22	3451	+2.0	21	34	36	136	−16	15	30	+482	21	23	20
	13	16	3527	+1.6	23	09	02	134	− 9	19	11	+692	15	30	14
	13	19	3532	+1.6	23	15	45	134	− 8	44	17	+703	18	30	43
	20	19	3530	−1.1	5	48	22	149	+20	38	56	+200	18	58	19
	23	23	3449	−1.3	8	52	57	139	+18	29	48	−376	23	10	48
	30	14	3267	−0.7	14	16	07	114	− 8	20	01	−612	14	36	56
October	3	15	3248	+0.3	16	39	14	122	−18	21	56	−347	15	48	55
	6	15	3257	+0.7	19	11	34	131	−21	22	11	+ 66	16	00	45
	7	18	3358	+1.9	20	10	59	133	−20	12	57	+242	19	05	11
	9	17	3452	+2.3	21	55	23	133	−15	06	27	+534	18	12	54
	21	21	3426	−1.7	9	30	48	133	+16	44	53	−471	23	00	52

If α denotes the right ascension of the star the hour angle is given by

$$h = \text{LST} - \alpha \qquad \text{...(2)}$$

where LST is the local sidereal time at the instant under consideration. We list in the last column of Table 2 the Greenwich Sidereal Time (GST) for a few selected hours on a few days of interest. An observer at a longitude λ east of Greenwich can obtain his local sidereal time at the corresponding times by adding his longitude to the GST :

$$\text{LST} = \text{GST} + \lambda. \qquad \text{...(3)}$$

The sidereal time at any other instant can be obtained by noting that in one hour of solar time the sidereal time changes by $1^h\ 0^m\ 09^s.856$, or in one day the sidereal time gains $3^m 56^s.558$ over the solar time. As an example consider an observer at a longitude 77° east of Greenwich. The longitude can be converted to hours by simply dividing by it 15. Thus the observer's longitude is $5^h\ 8^m$ E. Referring to Table 2, his LST at 13^h UT on July 4 is $7^h\ 49^m\ 49^s + 5^h\ 8^m\ 0^s = 12^h\ 57^m\ 49^s$. An hour later ($14^h$ UT) his LST is $13^h\ 57^m\ 59^s$ and an hour earlier (12^hUT) it is $11^h\ 57^m\ 39^s$. We now proceed to simulate the occultation on a graph sheet. We draw the x- and y-axes with the origin near the centre of the sheet and draw a circle of 0.2725 units with its centre at the origin of the axes. This circle is the shadow of the moon on the fundamental plane and its radius is in the units of the radius of the earth. The co-ordinates of the centre of the moon's shadow are given by

$$x = \frac{15}{p_1} (\alpha_1 - \alpha) \cos \delta_1 \qquad \text{...(4)}$$

$$y = \frac{(\delta_1 - \delta)}{p_1} \qquad \text{...(5)}$$

Here p_1 is the maximum horizontal parallax of the moon, (α, δ) the coordinates of the star and (α_1, δ_1), of the moon. In equations (4) and (5), p_1 and $(\delta_1 - \delta)$ are in seconds of arc and $(\alpha_1 - \alpha)$ in seconds of time. Table 2 lists the values of p_1, α_1 and δ_1 for specific times on specific days as also their mean hourly rates of change, $\Delta p_1/\Delta t$, $\Delta\alpha_1/\Delta t$ and $\Delta\delta_1/\Delta t$. The projection on the fundamental plane of the position of the observer is then calculated using the following equations:

$$\xi = \rho \cos \phi \sin h \qquad \text{...(6)}$$

$$\eta = \rho (\cos \delta \sin \phi - \sin \delta \cos \phi \cos h) \qquad \text{...(7)}$$

where ϕ denotes the latitude of the observer and the hour angle h is calculated from equation (2). The geocentric distance ρ is in the units of earth's equatorial radius. Now the position of the observer with respect to the shadow of the moon is given by

$$f = x - \xi \qquad \text{...(8)}$$

and

$$g = y - \eta. \qquad \text{...(9)}$$

The values of f and g are calculated for the nearest hour at which α_1 and α coincide and also for one or two hours on either side of this probable hour of occultation.

The points are joined to give the apparent path of the observer with respect to the shadow of the moon. If this path intersects the circle denoting the moon an occultation takes place and the actual time can be obtained by interpolating in time the point of intersection on the path of the observer. One may use the above method to compute more accurate times if one calculates x', y', the hourly rates of change of x and y. If f and g are calculated for a time t, the actual time of occultation is a time Δt later :

$$\Delta t = \frac{(0.2725)^2 - f^2 - g^2}{2\,[f x' + g y' - 0.2625 a_0]} \qquad \ldots(10)$$

where

$$a_0 = f \cos \phi \cos h + g\, \xi \sin \delta. \qquad \ldots(11)$$

One can improve the accuracy by improving the estimated time as $t_1 = t + \Delta t$ and then proceeding to calculate the further correction $\triangle t_1$ to the estimated time from equation (10) using the new values of f, g, x', y' and a_0. The calculations can be repeated until the desired accuracy is attained.

As an illustration of the method we proceed to check whether an observer in Bombay would see o Sagittarii being occulted by the moon on August 12. The longitude of Bombay is 72° 49′E or $4^h51^m16^s$E while the latitude is +18° 54′. Hence $\sin \phi = 0.3239$ and $\cos \phi = 0.9461$. The geocentric distance of Bombay is 0.9936 in the units of the mean equatorial radius. We will assume this to be unity in the following calculations. This approximation, as also the approximate coordinates assumed above, limit the accuracy of the computations to about one minute in time. The coordinates of o Sagittarii for 1981 are $\alpha = 19^h\ 3^m\ 34^s$ and $\delta = -21°46'$. Hence we have $\rho \cos \delta \sin \phi = 0.3008$ and $\rho \sin \delta \cos \phi = -0.3508$. From Table 2 we notice that the right ascensions of moon and of o Sagittarii coincide a little after 18^hUT on August 12. Therefore we proceed to calculate the position of the observer with respect to the shadow at 17^h, 18^h and 19^h UT (Table 3). The results are shown in Figure 2. The observer intersects the shadow between 18^h (B) and 19^h (C) at the point D. The time of disappearance can be obtained by adding the ratio BD/BC= $0^h.29$ to 18^h UT. We may alternately use equation (10) with the mean values x'= 0.5829 and $y' = 0.0115$ at 18^h UT and obtain $\Delta t = -0.0731/-0.2522 = 0^h.2898$. Thus the time of disappearance is $18^h\ 17^m.4$ UT. Extending the calculation for 20^h UT would yield the time of reappearance, which we leave as an exercise for the reader. The answer is $19^h\ 33^m$ as seen in Figure 2.

The star o Sagittarii does not appear in Table 2 since it just misses the southern edge of the moon as seen from Kavalur. That is, Kavalur is a little south of the path of the shadow.

2. Observing meteors

Meteors or 'shooting stars' are the trails of small particles (meteoroids) which fall on the earth from outer space and burn because of the friction with the atmosphere. The meteoroids generally burn completely before they reach the earth's surface. Occasionally we may have a larger chunk of matter that does not burn fully and thus we have *meteorites* falling on the earth. The case of the Dhajala meteorite shower on 1976 January 28 in Gujarat is such an example.

Table 3. Sample calculation for the prediction of lunar occultations.
Occultation of o Sagittarii on 1981 August 12 : Longitude (λ) = 72° 49′E; Latitude (ϕ) = +18° 54′; cos ϕ = 0.9461; sin ϕ = 0.3239; ρ cos δ sin ϕ = 0.3008; $_{0}$ sin δ cos ϕ =0.3508

		17h			18h			19h	
α_1	19	01	01	19	03	15	19	05	29
α	19	03	34	19	03	34	19	03	34
$\alpha_1-\alpha$	− 0	2	33	−0	019		+0	2	5
$(\alpha_1-\alpha)$ sec		−153			− 19			+125	
δ_1	−21	06	30	−21	05	51	−21	05	12
δ	−21	46		−21	46		−21	46	
$\delta_1-\delta$	0	39	30	0	40	09	0	40	48
$(\delta_1-\delta)$ arcsec		2370			2409			2448	
cos δ_1		0.9329			0.9330			0.9330	
p arcsec		−3336			3337			3338	
x		−0.6418			−0.0797			0.5241	
y		0.7104			0.7219			0.7334	
GST	14	24	14	15	24	24	16	24	34
λ	4	51	16	4	51	16	4	51	16
LST	19	15	30	20	15	40	21	15	50
h	0	14	29	1	12	25	2	10	21
h deg		3.6208			18.1042			32.5875	
ξ		0.0597			0.2940			0.5095	
η		0.6509			0.6342			0.5964	
f		−0.7015			−0.3737			0.0146	
g		0.0595			0.0877			0.1370	
a_0		−0.6637			−0.3456			−0.0142	
x'				0.5621	(0.5829)	0.6038			
y'				0.0115	(0.0115)	0.0115			

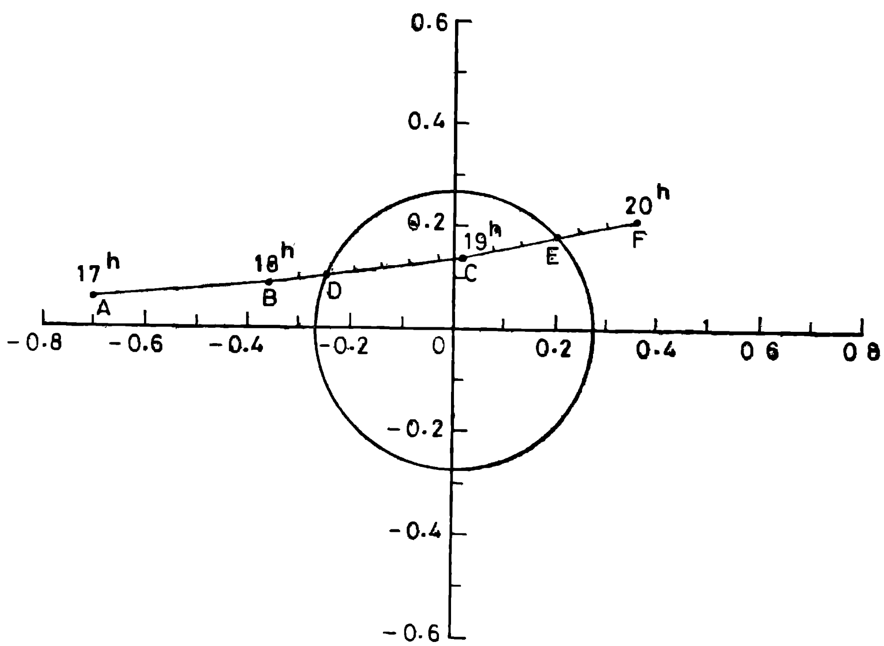

Figure 2. Position of a Bombay-based observer with respect to the shadow of the moon due to o Sagittarii on 1981 August 12. The positions at 17h(A), 18h(B), 19h(C) and 20h(F) UT are indicated. The distances BC and CF are divided equally in 6 parts, each of 10m intervals. The disappearance (D) takes place at 18h 17m.4 UT, and the reappearance (E) is at 19h 33m.3 UT.

On any clear moonless night we can observe a few meteors darting across the sky every hour. The hourly rate of the meteors increases with local time during any night. We observe twice as many meteors after midnight as we observe before midnight. The cause for this increase is that the observer is in the leading portion of earth in its orbit and sweeps past the particles scattered in space.

The period from June to December witnesses twice as many meteors as the first half of the year. This is because the earth passes close to the paths of several swarms of meteoroids orbiting about the sun. These swarms are the debris left over by dead or dying comets along their orbits. Meteors originating from an individual swarm give rise to a *meteor stream*. All the meteors belonging to one stream seem to diverge from a fixed point (the radiant) with respect to the stars. This point is the direction of the swarm with respect to the earth. Hence the radiant shift slowly as the earth approaches the swarm, becomes very diffuse at the time of maximum activity and continues to shift as the earth recedes from it.

Some meteor streams show a higher degree of activity while others can barely be recognised on the background of the sporadic meteors. Some of the streams have shown very spectacular displays in the past. The Leonid shower of November 12 showed about a thousand meteors every minute at its peak of activity in 1833. Such displays occur when a lump of very high particle density approaches the earth in its orbit which may have a period of several years, decades or even centuries. The physical properties and orbital speeds of different meteor streams are different depending on their parent comet. Thus the colour, speed and brightness of the meteors belonging to different meteor streams carry the signatures of their membership. The Andromedes of November are slow meteors and leave yellowish trains of sparks behind them. The Leonids of the same month on the other hand, move very swiftly but leave phosphorescent trails.

Table 4 lists some of the meteor streams visible between July and October. The streams are generally known after the constellation in which their radiant lies. When different streams have their radiants in same constellation a better specification is given. The epoch in column 2 is the epoch of maximum activity while the limits in the next column give the period during which the stream is active. The maximum hourly rate of meteors is the rate one may expect if the radiant were overhead on a clear moonless night at the peak activity of the stream. The coordinates of the radiant appear in the next two columns of the table. The age of the moon (new moon = 0) appears in the seventh column and the local time of transit of the radiant in the eigth followed by remarks on some of the streams. The meteors are observed more easily near the new moon rather than when the moon is bright.

Unfortunately the Perseids are returning near full moon this year. The Perseids have been showing an increased activity in the last few years since the associated comet Swift-Tultle (1862 III) with a period of 120 years is expected to return shortly. There are a few hours left after moon set on August 12 and on earlier days when we can expect to see a spectacular display. The Capricornids of August have a favourable moon this year. This minor shower which shows only a few meteors per hour is known for the yellow fireballs associated with it. Fireballs are meteors which keep burning until they reach very close to the surface of the earth and reach a brightness that may rival the moon's. Though the α Capricornid stream is attributed to the comet Honda-Mrkos-Pajdusakova, it may be a conglomeration of

Table 4. Some meteor streams active between 1981 July and October

Stream	Epoch	Limits	Max. hourly rate	Radiant h	Radiant m	Radiant deg	Age of Moon d	Local time of transit h	Remarks
Capricornids	July 25	July 10–Aug. 15	6	21	00	−15	23	1	Bright meteors
S δ Aquarids	July 27	July 15–Aug. 15	20	22	36	−17	25	2	
Pisces Australids	July 30	July 15–Aug. 20	8	22	40	−30	28	2	
α Capricornids	Aug. 1	July 15–Aug. 25	8	20	36	−10	1	0	Yellow fireballs
Perseids	Aug. 12	July 25–Aug. 18	68	3	04	+58	12	6	many bright flaring meteors; fine trains
N δ Aquarids	Aug. 12	July 14–Aug. 25	20	22	36	00	12	1	
κ Cygnids	Aug. 19	Aug. 9–Oct. 6	4	19	20	+55	19	22	
N ι Aquarids	Aug. 20	July 15–Sept. 20	6	22	04	−06	20	0	
Orionids	Oct. 20	Oct. 165–Oct. 26	30	6	24	+15	22	6	Multiple radiants; fine trains

Additional list of minor streams :

Stream	Epoch	Limits
S. Piscids	Sept. 20	Aug. 31–Nov. 2
Annual Andromedids	Oct. 3	Sept. 25–Nov. 12
N. Piscids	Oct. 12	Sept. 25–Oct. 19
N. Taurids	Nov. 13	Sept. 19–Dec. 1

several independent streams as witnessed by the multiple radiant and several peaks in its activity. Apart from a peak epoch on August 1 it has two other peaks at July 26 and August 7. The Orionids of October have a multiple radiant too.

An observer of meteors plots the apparent path of the meteors with respect to bright stars. This helps him isolate the members of an individual stream from the sporadic meteors that keep darting across the sky at a low hourly rate. The hourly rate of meteors belonging to the stream are then counted for a given hour and date. One may estimate the brightness of each meteor on the stellar magnitude scale and derive a luminosity function (number of meteors of a given magnitude). The altitude of the radiant, the conditions of the sky and the altitude and the phase of the moon are needed for an effective intercomparison of data obtained at different times and by different observers. A description of the appearance, colour of the meteor and the trails left by it helps in the recognition of the special characteristics of the individual streams.

The plots of meteor paths collected over a few hours are needed for a recognition of the minor streams. There are several suspected streams which one can verify utilizing such plots. The following suspected streams are not well established yet Pegasids on August 12; an as yet unnamed meteor shower around September 16–18 with a radiant at $19^h 00^m +25°$; and the δ Aurigids on October 15–16 with a radiant at $6^h25^m + 52°.5$ (12° NE of Capella) predicted by NASA-NMSU Meteor Observatory. There may be several minor meteor streams which are still awaiting discovery.

3. Planetary phenomena

Mercury attains greatest eastern elongation on July 14 and can be seen above the eastern horizon before sunrise. It is too close to sun to be seen in August, the superior conjunction being on August 10. It reappears in the western sky in the evening of September and can be seen barely 0°.4 away from Spica on July 20. It is lost in the solar glare again in October, the inferior conjunction being on October 18.

Venus is an evening object from July to October. As it approaches the sun it will be successively more and more difficult to observe. It passes through the Praesepe (bee-hive) cluster in Cancer on July 23, north of spica on September 6 and north of Antares on October 17 and on its course, passes close to Saturn (August 25), Jupiter (August 27), Uranus (October 7) and Neptune (October 29).

Mars moves from Taurus in July, to Leo in October and can be seen for a few hours before sunrise. It passes south of Castor and Pollux on August 22. It will provide an interesting sight between August 24–26 with a crescent moon also nearby. Mars passes north of Regulus on October 19.

Jupiter is close to η Virginis on July 21–22. Saturn is also in Virgo. Jupiter approaches Saturn till the end of July when their separation reaches 1°.2, and begins to recede thereafter. Both the planets will be low in the western sky after the sunsets of August-September and set with the sun in October.

Uranus is in Libra. It passes barely one arcmin west of 41 Librae on September 12–13 and 12 arcmin north of κ Librae on October 1. It is a little brigher than the sixth magnitude.

Neptune is a little brighter than the eigth magnitude in the constellation of Ophiuchus, about 2° southeast of ξ Ophiuchi. It is not easy to spot in the crowded field of the Milky Way.